Improved lattice Boltzmann model for incompressible two-dimensional steady flows

Zhifang Lin, Haiping Fang, and Ruibao Tao
T. D. Lee Physics Laboratory and Department of Physics, Fudan University, Shanghai 200433, China
(Received 26 June 1996)

An improved lattice Boltzmann model with single time relaxation has been proposed for incompressible two-dimensional (2D) steady flows. In the improved model, the steady-state incompressible Navier-Stokes equations can be recovered in exact form and the density of the fluid becomes an irrelevant invariant, satisfying the requirement of incompressibility. Exact analytical solutions to the distribution functions of the 2D triangular and square lattice Boltzmann models have been obtained for steady plane Poiseuille flow based on the present scheme. Boundary conditions that can be used to recover exactly such analytical solutions in numerical simulations are proposed. [S1063-651X(96)07312-6]

PACS number(s): 47.10.+g, 05.50.+q

I. INTRODUCTION

In recent years, the lattice Boltzmann (LB) method [1–4] has achieved great success for simulation of various transport phenomena ranging from multiphase fluid flows [5,6] to fluid flows through porous media [7–9] and chemical reacting flows [10]. In particular, the LB method as a tool for modeling isothermal, incompressible, low-Reynolds-number viscous flow seems most promising. Among different LB methods, the model with single time relaxation, usually referred to as the lattice Boltzmann Bhatnagar-Gross-Krook (LBGK) model [3,4], is believed to be more robust and most simple. In practice, however, when simulating the incompressible flows, the steady-state macroscopic equations recovered from the conventional LBGK model are different from the steady-state incompressible Navier-Stokes equations by terms of spatial derivatives of the fluid density ρ. The discrepancies are the so-called compressibility errors in the LB model, which cannot be eliminated by the refinement of the lattice or by decreasing the viscosity without sacrificing the stability [11]. In addition, according to the equation of state from the LBGK model, the pressure p is related to the fluid density ρ by $p=c_s^2\rho$, with c_s, the speed of sound, being a constant. For the incompressible fluid, the requirement that ρ be a constant in space results in a constant pressure throughout the flow, which is inconsistent with many practical applications, such as flow driven by the pressure difference like Poiseuille flow.

Some authors have noticed these problems. On the one hand, in their improved LBGK model on the square lattice for incompressible steady flow, Zou and co-workers [11] have recovered the exact form of the Navier-Stokes equations by using a modified local equilibrium distribution and redefined velocity. However, the constant density for incompressible flow with a pressure gradient still violates the equation of state $p=c_s^2\rho$. On the other hand, by replacing the pressure gradient by a uniform body force, exact analytical solutions to the distribution functions of the LBGK model for steady Poiseuille flow have been obtained [12] on two-dimensional (2D) triangular and square lattices with a constant fluid density ρ. Nevertheless, the introduction of a uniform body force to replace the pressure gradient seems rather artificial since the pressure gradient through the flow field is not necessarily a constant, especially for complex geometry.

In this paper, an improved LBGK model is proposed that can both recover the exact form of 2D steady-state incompressible Navier-Stokes equations and eliminate the inconsistency between the constant density and variable pressure. Our scheme is illustrated on a 2D triangular lattice as well as a square lattice. Based on the present scheme, exact analytical solutions to the distributions functions of 2D triangular- and square-lattice LBGK models for steady-state Poiseuille flow are obtained. Unified boundary conditions that can be used to obtain the analytical solutions to the distribution functions are proposed for numerical simulation on both lattices. On the square lattice, different analytical solutions to the microscopic distribution functions of the LBGK model with the same macroscopic quantity due to different boundary conditions are briefly discussed.

II. TRIANGULAR LBGK MODEL

A. Analytical solution

Let us first illustrate the improved LBGK model on a triangular lattice with seven types of lattice links $\vec{e}_i=[\cos(i-1)\pi/6,\sin(i-1)\pi/6]$, for $i=1,\ldots,6$ and $\vec{e}_0=0$ (see Fig. 1). The improved LBGK model is considered as the

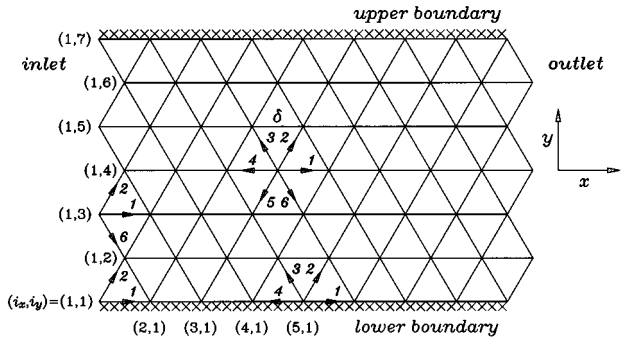

FIG. 1. Schematic plot of the geometry for the plane channel flow on the triangular lattice with $n_x=9$ and $n_y=7$. Here n_x and n_y are the numbers of lattice points in the x and y directions, respectively.

equation for the evolution of $f_i(\vec{x},t)$,

$$f_i(\vec{x}+\delta\vec{e}_i,t+\delta)-f_i(\vec{x},t)=-\frac{1}{\tau}[f_i(\vec{x},t)-f_i^{(0)}(\vec{x},t)],$$

$$i=0,1,\ldots,6, \quad (1)$$

where $f_i(\vec{x},t)$ is the distribution function representing the probability of finding a ''momenton'' with momentum $\vec{e}_i$ at node $\vec{x}=(x,y)$ and time t, and $f_i^{(0)}(\vec{x},t)$ is the corresponding equilibrium distribution. The right-hand side of Eq. (1) represents the collision term and τ is the single relaxation time that controls the rate of approach to equilibrium [3,4]. The macroscopic flow velocity $\vec{u}$ is defined in terms of the distribution function by

$$\rho\vec{u}=\sum_{i=1}^{6} f_i\vec{e}_i, \quad (2)$$

where ρ is the constant fluid density and is set to unity for an *incompressible* fluid.

The equilibrium distribution functions of momentum are supposed to be dependent only on the local flow velocity $\vec{u}$. A suitable choice is [11]

$$f_0^{(0)}=\alpha d-\vec{u}\cdot\vec{u},$$

$$f_i^{(0)}=\frac{(1-\alpha)d}{6}+\frac{1}{3}(\vec{e}_i\cdot\vec{u})+\frac{2}{3}(\vec{e}_i\cdot\vec{u})^2-\frac{1}{6}\vec{u}\cdot\vec{u},$$

$$i=1,\ldots,6, \quad (3)$$

where α is an adjustable parameter, usually chosen as 1/2, and d is given by

$$\sum_{i=0}^{6} f_i^{(0)}=\sum_{i=0}^{6} f_i=d.$$

That is, the idea is to let momentum propagate and collide rather than fluid particles themselves, because for the case of an incompressible fluid, the density is an irrelevant invariant and set to unity. Note that Eq. (1) is written in physical units with the value of the lattice link being δ and the speed for the particle on the lattice being unity. As a result, a time step also has the value of δ.

A Chapman-Enskog procedure can be applied to (1) to derive the macroscopic equations of the model. For the steady case, they can be worked out as

$$\partial_\alpha u_\alpha=0 \quad (4)$$

and

$$\partial_\beta(u_\alpha u_\beta)=-\partial_\alpha p+\nu\partial_\beta\partial_\beta u_\alpha, \quad (5)$$

which is the exact form of the steady incompressible Navier-Stokes equations at constant density $\rho=1$. In the above equations, the Einstein summation convention has been used and the pressure and the kinematic viscosity are given, respectively, by

$$p=\frac{(1-\alpha)d}{2}, \quad \nu=\frac{(2\tau-1)\delta}{8}. \quad (6)$$

It can be seen from the expression of pressure that the inconsistency has been eliminated between the constant density ρ and variable pressure p related by the equation of state $p=c_s^2\rho$ in the conventional LBGK model.

As a first application of the improved LBGK model for steady-state incompressible fluid, let us consider the plane Poiseuille flow in a channel with width $2L$ and velocity $\vec{u}=(u_x,u_y)=(u,0)$, which is an exact solution of the incompressible Navier-Stokes equations (4) and (5) and is given by

$$u=u_0\left(1-\frac{y^2}{L^2}\right), \quad \frac{\partial p}{\partial x}=-G, \quad \frac{\partial p}{\partial y}=0, \quad (7)$$

where G is a constant associated with the characteristic velocity u_0 by

$$G=2\rho\nu u_0/L^2. \quad (8)$$

Without loss of generality, we may assume that $L=1$, which can be achieved by a scaling of $y'=y/L$.

Now suppose that the improved LBGK model can model Poiseuille flow without compressibility error. Then there must be a solution $f_i(\vec{x},t)$ to Eq. (1) that represents the Poiseuille flow. The solution $f_i(\vec{x},t)$ is expected to have the following properties: (i) $f_i(\vec{x},t)$ is steady, i.e., $f_i(\vec{x},t)=f_i(\vec{x})=f_i(x,y)$ is independent of time t; (ii) $\Sigma_{i=0}^{6} f_i(\vec{x})=d=d_c(1-gx)$, where d_c is a constant and g is related to constant pressure gradient by

$$g=\frac{4\nu u_0}{(1-\alpha)d_c}, \quad (9)$$

according to (7) and (8) (remember that $L=1$ and $\rho=1$); (iii) $f_2(x,y)=f_6(x,-y)$ and $f_3(x,y)=f_5(x,-y)$ due to the symmetry of the flow (see Fig. 1); (iv) $\Sigma_{i=1}^{6} f_i(x,y)e_{iy}=u_y=0$; and (v) $\Sigma_{i=1}^{6} f_i(x,y)e_{ix}=u_x=u$, where $u=u_0(1-y^2)$ (recall that $L=1$).

In the following we shall find such a solution. From (3), the equilibrium distributions for momentum reduce to, for $u_x=u$ and $u_y=0$,

$$f_0^{(0)}(x,y)=\alpha d-u^2,$$

$$f_1^{(0)}(x,y)=\frac{(1-\alpha)d}{6}+\frac{1}{3}u+\frac{1}{2}u^2,$$

$$f_4^{(0)}(x,y)=\frac{(1-\alpha)d}{6}-\frac{1}{3}u+\frac{1}{2}u^2, \quad (10)$$

$$f_2^{(0)}(x,y)=\frac{(1-\alpha)d}{6}+\frac{1}{6}u, \quad f_3^{(0)}(x,y)=\frac{(1-\alpha)d}{6}-\frac{1}{6}u,$$

$$f_5^{(0)}(x,y)=\frac{(1-\alpha)d}{6}-\frac{1}{6}u, \quad f_6^{(0)}(x,y)=\frac{(1-\alpha)d}{6}+\frac{1}{6}u.$$

Suppose the solution $f_i(x,y)$ to be of the form

$$f_i(x,y)=(a_i'd+a_i+b_iy+c_iy^2+d_iy^3+e_iy^4) \quad \text{for } i=0,1,4, \tag{11}$$

$$f_i(x,y)=(a_i'd+a_i+b_iy+c_iy^2) \quad \text{for } i=2,3,5,6,$$

where, for $i=2,3,5,6$, $f_i(x,y)$ are expected to be dependent on y up to y^2 terms because the corresponding $f_i^{(0)}$ is a linear function of u. In Eqs. (11) the 34 coefficients a_i', a_i, b_i, c_i, etc., are supposed to be independent of y. With the assumption (11), one is ready to find the coefficients by using the steady condition, while the other four properties of f_i serve to confirm the correctness of the form (11).

In order that $f_i(\vec{x},t)$ be steady, for $f_0(\vec{x})$ one should have

$$f_0^+(x,y)=f_0(x,y)-\frac{1}{\tau}[f_0(x,y)-f_0^{(0)}(x,y)]=f_0(x,y). \tag{12}$$

Here f_i^+ denote the distribution function immediately after collision. Substituting Eqs. (10) and (11) into (12) yields

$$a_0'=\alpha, \quad a_0=-u_0^2, \quad b_0=d_0=0, \quad c_0=2u_0^2, \quad e_0=-u_0^2. \tag{13}$$

The steady condition of $f_1(\vec{x})$ requires

$$f_1^+(x,y)=f_1(x,y)-\frac{1}{\tau}[f_1(x,y)-f_1^{(0)}(x,y)]=f_1(x+\delta,y), \tag{14}$$

from which it follows that

$$a_1'=\frac{1-\alpha}{6}, \quad a_1=\frac{1}{3}u_0+\frac{1}{2}u_0^2+\frac{2}{3}\tau\nu u_0\delta, \tag{15}$$

$$b_1=d_1=0, \quad c_1=-\frac{1}{3}u_0-u_0^2, \quad e_1=\frac{1}{2}u_0^2.$$

Similarly, for $f_2(\vec{x})$ to be steady, one expects

$$f_2^+(x,y)=f_2(x,y)-\frac{1}{\tau}[f_2(x,y)-f_2^{(0)}(x,y)] =f_2(x+\delta/2,y+\delta_y), \tag{16}$$

where $\delta_y=\sqrt{3}\delta/2$. As a result, one has the coefficients

$$a_2'=\frac{1-\alpha}{6}, \quad a_2=u_0+\frac{1}{3}\tau\nu u_0\delta+\frac{1}{8}\tau u_0\delta^2-\frac{1}{4}\tau^2u_0\delta^2, \tag{17}$$

$$b_2=\frac{1}{3}\tau u_0\delta_y, \quad c_2=-\frac{1}{6}u_0.$$

Other coefficients can be found in a similar way (the final results are summarized below)

$$f_0(x,y)=\alpha d-u^2,$$

$$f_1(x,y)=\frac{(1-\alpha)d}{6}+\frac{1}{3}u+\frac{1}{2}u^2+\frac{2}{3}\tau\nu u_0\delta,$$

$$f_4(x,y)=\frac{(1-\alpha)d}{6}-\frac{1}{3}u+\frac{1}{2}u^2-\frac{2}{3}\tau\nu u_0\delta,$$

$$f_2(x,y)=\frac{(1-\alpha)d}{6}+\frac{1}{6}u+\frac{1}{3}\tau u_0y\delta_y-\frac{2}{3}\tau\nu u_0\delta, \tag{18}$$

$$f_3(x,y)=\frac{(1-\alpha)d}{6}-\frac{1}{6}u-\frac{1}{3}\tau u_0y\delta_y+\frac{2}{3}\tau\nu u_0\delta,$$

$$f_5(x,y)=\frac{(1-\alpha)d}{6}-\frac{1}{6}u+\frac{1}{3}\tau u_0y\delta_y+\frac{2}{3}\tau\nu u_0\delta,$$

$$f_6(x,y)=\frac{(1-\alpha)d}{6}+\frac{1}{6}u-\frac{1}{3}\tau u_0y\delta_y-\frac{2}{3}\tau\nu u_0\delta.$$

It can be easily shown that (18) satisfies properties (i)–(v). It is, therefore, at least one exact representation of the distribution functions for the Poiseuille flow.

B. Boundary conditions

The next problem is to check whether the numerical simulation can recover the analytical solution (18). To do so, the boundary conditions are very important. As it is well known, the implementation of an inappropriate boundary condition may cause a first-order error [12–15]. In our numerical simulation, we adopt the nonslip boundary conditions for lower and upper boundaries proposed by Noble *et al.* [14], while another approach for the boundary with prescribed pressure is presented that can be used to obtain the analytical results (18) up to machine accuracy [15].

1. Nonslip boundary condition

To cast the nonslip boundary condition at lower or upper boundaries, we use the following scheme proposed in [14]. For simplicity, we take the case of a bottom node as an example. A similar procedure can be applied to the top node. The boundary is in the x direction with $\vec{e}_5$ and $\vec{e}_6$ pointing into the wall for the bottom node [see, e.g., node (5,1) in Fig. 1]. After streaming, f_0, f_1, f_4, f_5, and f_6 are known, while f_2 and f_3 are unknown. For the nonslip boundary, $u_x=u_y=0$ are specified on the wall and we have to determine f_2, f_3, and d from (2). So we have the equations

$$f_0+f_1+f_2+f_3+f_4+f_5+f_6=d,$$

$$f_1+(f_2+f_6)/2-f_4-(f_3+f_5)/2=u_x=0, \tag{19}$$

$$(\sqrt{3}/2)[f_2+f_3-(f_5+f_6)]=u_y=0,$$

from which f_2, f_3, and d can be worked out as

$$f_2=f_5-(f_1-f_4),$$

$$f_3=f_6+(f_1-f_4), \tag{20}$$

$$d=f_0+f_1+f_4+2f_5+2f_6.$$

With (20), the relaxation step can be applied on the boundary nodes as well. Notice that although the present nonslip boundary conditions are in the same form as those proposed in [14], the meaning is rather different, because in the present model f_i is no longer a fluid particle distribution. The boundary conditions in [14] suffer the disadvantage of nonconservation of the particle number on boundaries, so they seem to apply only for a somewhat permeable boundary wall. On the other hand, in our model, as f_i is related to momentum (or velocity) instead of particle distribution, they are not necessarily a conserved quantity on boundaries. The nonslip boundary conditions in the present LBGK model therefore may be applied to an impermeable boundary.

2. Boundary with prescribed pressure

For the Poiseuille flow driven by pressure difference, the pressure at the inlet and outlet for the flow are specified. To cast the boundary condition with the specification of pressure at the inlet and outlet of the channel, we use the following scheme. For simplicity, we consider the case of a node at the inlet [see, e.g., node (1,3) in Fig. 1]. A similar procedure can be applied to the nodes at the outlet. The boundary with specified pressure is supposed to align in the y direction with $\vec{e}_3$, $\vec{e}_4$, and $\vec{e}_5$ pointing outside the system of interest on a node at the inlet (see Fig. 1). After streaming, f_0, f_3, f_4, and f_5 are known, while f_1, f_2, and f_6 are unknown. For a node at the inlet, $u_y=0$ is specified and d is also known from Eq. (6) since the pressure is specified. So we have to determine f_1, f_2, f_6, and u_x from (2), namely,

$$\begin{aligned} &f_0+f_1+f_2+f_3+f_4+f_5+f_6=d,\\ &f_1+(f_2+f_6)/2-f_4-(f_3+f_5)/2=u_x,\\ &(\sqrt{3}/2)[f_2+f_3-(f_5+f_6)]=u_y=0. \end{aligned} \tag{21}$$

There are four unknown quantities f_1, f_2, f_6, and u_x, while only three equations are available from (2). We assume the following equation for the prescribed pressure boundary:

$$f_1+f_4=f_1^{(0)}+f_4^{(0)}. \tag{22}$$

The effect of this rule can be understood as the cancellation of the nonequilibrium part in the direction normal to the inlet (see Fig. 1). From Eqs. (21) and (22), f_1, f_2, f_6, and u_x can be worked out as

$$\begin{aligned} u_x&=1-\sqrt{1-S_1},\\ f_1&=S_2-f_4,\\ f_2&=\frac{1}{2}(d-f_0-S_2)-f_3,\\ f_6&=\frac{1}{2}(d-f_0-S_2)-f_5, \end{aligned} \tag{23}$$

where

$$\begin{aligned} S_1&=d-(f_0+2f_3+4f_4+2f_5)+\frac{(1-\alpha)d}{3},\\ S_2&=f_1^{(0)}+f_4^{(0)}=\frac{(1-\alpha)d}{3}+u_x^2. \end{aligned} \tag{24}$$

Now let us turn to a corner node at the inlet. Consider the bottom node at the inlet as an example [see node (1,1) in Fig. 1]. After streaming, only three f's, i.e., f_0, f_4, and f_5, are known. But, in addition to d and $u_y=0$, $u_x=0$ is also specified at the corner node. As a result, the four unknown quantities, f_3 as well as f_1, f_2, and f_6, are also given by (23) and (24) with $u_x=0$ and

$$f_3=\frac{d-f_0}{2}+\frac{(1-\alpha)d}{6}-f_5-2f_4. \tag{25}$$

A similar procedure can be applied to the top node at the inlet.

There are still two points that need to be mentioned. In our simulation, the triangular lattice is constructed as shown in Fig. 1. For layers with odd and even values of i_y, the x coordinates are different even with the same value of i_x [see, e.g., nodes (1,1) and (1,2) in Fig. 1]. So in our simulation, after n_x, d_1, and d_2 are specified, where n_x is the number of lattice points in the x direction and d_1 and d_2 are the values of d on nodes at the inlet and outlet with odd values of i_y, respectively, we cast $d=d_1$ (d_2) on the nodes at the inlet (outlet) with odd values of i_y and $d=d_1-\delta_d$ $(d_2-\delta_d)$ on the nodes at the inlet (outlet) with even values of i_y. Here $\delta_d=(d_2-d_1)/(n_x-1)$. The second point is that in our numerical simulation, all nodes at the inlet (with $i_x=1$) or outlet (with $i_x=n_x$) are treated as boundary nodes by the boundary conditions mentioned above. That is, even for those nodes with even (odd) values of i_y at the inlet (outlet), f_2 and f_6 (f_3 and f_5) are supposed to be unknown and found by Eqs. (23) and (24), although they may be indeed known from streaming.

With the use of the boundary conditions described above, our numerical simulation shows that f_i evolve, accurately up to machine accuracy, into the analytical results (18) for τ ranging from 0.65 to 20.0, u_0 ranging from 0.001 to 0.3, and a variety of n_x and n_y, after several thousands of time steps, when the simulation becomes stable. Here n_x and n_y are the numbers of lattice points in the x and y directions, respectively.

III. SQUARE LBGK MODEL

A. Analytical solution

Now we turn to the square lattice. The LBGK model on the square lattice is the equation for the evolution of the momenton distribution function $f_i(\vec{x},t)$,

$$f_i(\vec{x}+\delta\vec{e}_i,t+\delta)-f_i(\vec{x},t)=-\frac{1}{\tau}[f_i(\vec{x},t)-f_i^{(0)}(\vec{x},t)], \quad i=0,1,\ldots,8, \tag{26}$$

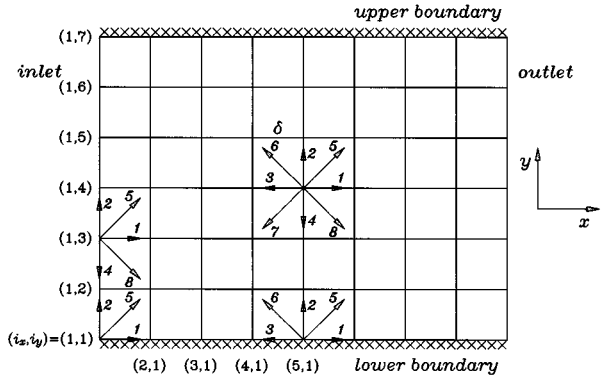

FIG. 2. Schematic plot of the geometry for the plane channel flow on the square lattice with $n_x=9$ and $n_y=7$. Here n_x and n_y are the numbers of lattice points in the x and y directions, respectively.

where $\vec{e}_0=0$, $\vec{e}_i=[\cos(i-1)\pi/2,\sin(i-1)\pi/2]$ for $i=1,2,3,4$, and $\vec{e}_i=\sqrt{2}[\cos(i-4-\frac{1}{2})\pi/2,\sin(i-4-\frac{1}{2})\pi/2]$ for $i=5,6,7,8$ (see Fig. 2). The macroscopic flow velocity $\vec{u}$ is defined in terms of $f_i(\vec{x},t)$ by

$$\rho\vec{u}=\sum_{i=1}^{8} f_i\vec{e}_i, \tag{27}$$

where the constant fluid density ρ is again set to unity for an *incompressible* fluid.

The equilibrium momentum distribution functions depend only on the local velocity $\vec{u}$. They can be chosen in the form [11]

$$f_0^{(0)}=\alpha d-\frac{2}{3}\vec{u}\cdot\vec{u},$$

$$f_i^{(0)}=\frac{(1-\alpha)d}{5}+\frac{1}{3}(\vec{e}_i\cdot\vec{u})+\frac{1}{2}(\vec{e}_i\cdot\vec{u})^2-\frac{1}{6}\vec{u}\cdot\vec{u}$$

$$\text{for } i=1,\ldots,4, \tag{28}$$

$$f_i^{(0)}=\frac{(1-\alpha)d}{20}+\frac{1}{12}(\vec{e}_i\cdot\vec{u})+\frac{1}{8}(\vec{e}_i\cdot\vec{u})^2-\frac{1}{24}\vec{u}\cdot\vec{u}$$

$$\text{for } i=5,\ldots,8,$$

where α is an adjustable parameter, usually chosen as 4/9, and d is given by

$$\sum_{i=0}^{8} f_i^{(0)}=\sum_{i=0}^{8} f_i=d.$$

A Chapman-Enskog expansion can be applied to (26) to derive the macroscopic equations of the model. For the steady case, they can be worked out as the exact form of the steady incompressible Navier-Stokes equation at constant density $\rho=1$ [see Eqs. (4) and (5)]. On the square lattice, however, the pressure and the kinematic viscosity are given by

$$p=\frac{3(1-\alpha)d}{5},\quad \nu=\frac{(2\tau-1)\delta}{6} \tag{29}$$

in place of (6).

Now suppose that there is a solution $f_i(\vec{x},t)$ to Eq. (26) and it represents the Poiseuille flow (7) exactly. The five properties of $f_i(\vec{x},t)$ mentioned in Sec. II still hold for the square-lattice LBGK model, except that properties (ii) and (iii) should be replaced by (ii′) $\Sigma_{i=0}^{8} f_i(\vec{x})=d=d_c(1-gx)$, where d_c is a constant and g is related to pressure gradient by

$$g=\frac{10\nu u_0}{3(1-\alpha)d_c}, \tag{30}$$

and (iii′) $f_2(x,y)=f_4(x,-y)$, $f_5(x,y)=f_8(x,-y)$ and $f_6(x,y)=f_7(x,-y)$ owing to the symmetry of flow.

With the assumption

$$f_i(x,y)=(a_i'd+a_i+b_iy+c_iy^2+d_iy^3+e_iy^4)$$

$$\text{for } i=0,1,\ldots,8, \tag{31}$$

where the 54 coefficients a_i', a_i, b_i, c_i, etc., are supposed to be independent of y, one is ready to find the analytical solution by using a similar procedure. The results are

$$a_0'=\alpha,\quad a_1'=a_2'=a_3'=a_4'=\frac{1-\alpha}{5},$$

$$a_5'=a_6'=a_7'=a_8'=\frac{1-\alpha}{20}; \tag{32}$$

$$a_0=-\frac{2}{3}u_0^2,\quad b_0=d_0=0,\quad c_0=\frac{4}{3}u_0^2,\quad e_0=-\frac{2}{3}u_0^2; \tag{33}$$

$$a_1=\frac{1}{3}u_0+\frac{1}{3}u_0^2+\frac{2}{3}\delta\tau u_0\nu,\quad b_1=d_1=0,$$

$$c_1=-\frac{1}{3}u_0-\frac{2}{3}u_0^2,\quad e_1=\frac{1}{3}u_0^2; \tag{34}$$

$$a_2=-\frac{1}{6}u_0^2-\frac{1}{3}\delta^2\tau u_0^2+\frac{1}{6}\delta^4\tau u_0^2+\frac{2}{3}\delta^2\tau^2u_0^2-\frac{7}{3}\delta^4\tau^2u_0^2+6\delta^4\tau^3u_0^2-4\delta^4\tau^4u_0^2,$$

$$b_2=-\frac{2}{3}\delta\tau u_0^2+\frac{2}{3}\delta^3\tau u_0^2-4\delta^3\tau^2u_0^2+4\delta^3\tau^3u_0^2, \tag{35}$$

$$c_2=\frac{1}{3}u_0^2+\delta^2\tau u_0^2-2\delta^2\tau^2u_0^2,\quad d_2=\frac{2}{3}\delta\tau u_0^2,\quad e_2=-\frac{1}{6}u_0^2;$$

$$a_3=-\frac{1}{3}u_0+\frac{1}{3}u_0^2-\frac{2}{3}\delta\tau u_0\nu,\quad b_3=d_3=0,$$

$$c_3=\frac{1}{3}u_0-\frac{2}{3}u_0^2,\quad e_3=\frac{1}{3}u_0^2; \tag{36}$$

$$a_5=\frac{1}{6}\delta\tau u_0\nu+\frac{1}{12}u_0+\frac{1}{12}\delta^2\tau u_0-\frac{1}{6}\delta^2\tau^2u_0+\frac{1}{12}u_0^2$$
$$+\frac{1}{6}\delta^2\tau u_0^2-\frac{1}{12}\delta^4\tau u_0^2-\frac{1}{3}\delta^2\tau^2u_0^2+\frac{7}{6}\delta^4\tau^2u_0^2$$
$$-3\delta^4\tau^3u_0^2+2\delta^4\tau^4u_0^2, \tag{37}$$

$$b_5=\frac{1}{6}\delta\tau u_0+\frac{1}{3}\delta\tau u_0^2-\frac{1}{3}\delta^3\tau u_0^2+2\delta^3\tau^2u_0^2-2\delta^3\tau^3u_0^2,$$

$$c_5=-\frac{1}{12}u_0-\frac{1}{6}u_0^2-\frac{1}{2}\delta^2\tau u_0^2+\delta^2\tau^2u_0^2,$$

$$d_5=-\frac{1}{3}\delta\tau u_0^2,\quad e_5=\frac{1}{12}u_0^2;$$

$$a_6=-\frac{1}{6}\delta\tau u_0\nu-\frac{1}{12}u_0-\frac{1}{12}\delta^2\tau u_0+\frac{1}{6}\delta^2\tau^2u_0+\frac{1}{12}u_0^2$$
$$+\frac{1}{6}\delta^2\tau u_0^2-\frac{1}{12}\delta^4\tau u_0^2-\frac{1}{3}\delta^2\tau^2u_0^2+\frac{7}{6}\delta^4\tau^2u_0^2$$
$$-3\delta^4\tau^3u_0^2+2\delta^4\tau^4u_0^2, \tag{38}$$

$$b_6=-\frac{1}{6}\delta\tau u_0+\frac{1}{3}\delta\tau u_0^2-\frac{1}{3}\delta^3\tau u_0^2+2\delta^3\tau^2u_0^2-2\delta^3\tau^3u_0^2,$$

$$c_6=\frac{1}{12}u_0-\frac{1}{6}u_0^2-\frac{1}{2}\delta^2\tau u_0^2+\delta^2\tau^2u_0^2,$$

$$d_6=-\frac{1}{3}\delta\tau u_0^2,\quad e_6=\frac{1}{12}u_0^2;$$

$$a_4'=a_2',\quad a_4=a_2,\quad b_4=-b_2,$$
$$c_4=c_2,\quad d_4=-d_2,\quad e_4=e_2,$$
$$a_7'=a_6',\quad a_7=a_6,\quad b_7=-b_6,$$
$$c_7=c_6,\quad d_7=-d_6,\quad e_7=e_6, \tag{39}$$
$$a_8'=a_5',\quad a_8=a_5,\quad b_8=-b_5,$$
$$c_8=c_5,\quad d_8=-d_5,\quad e_8=e_5.$$

Note that these results are exact. If one omits all terms of $O(\delta^2)$, $O(\delta^3)$, and $O(\delta^4)$, the coefficients turn out to be much simpler.

B. Boundary conditions

In our numerical simulation, we adopt the nonslip boundary conditions for lower and upper boundaries proposed by Zou and He [13], while an alternative approach for the boundary with pressure specified is presented.

1. Nonslip boundary condition

To cast the nonslip boundary condition at lower or upper boundaries, we use the following scheme proposed in [13]. For simplicity, we take the case of a bottom node as an example. A similar procedure can be applied to the top node. The boundary is in the x direction with $\vec{e}_4$, $\vec{e}_7$, and $\vec{e}_8$ pointing into the wall for the bottom node [see, e.g., node (5,1) in Fig. 2]. After streaming, f_0, f_1, f_3, f_4, f_7, and f_8 are known, while f_2, f_5, and f_6 are unknown. For the nonslip boundary, $u_x=u_y=0$ are specified on the wall and we have to determine f_2, f_5, f_6, and d from (27). So we have the equations

$$f_0+f_1+f_2+f_3+f_4+f_5+f_6+f_7+f_8=d,$$
$$(f_1+f_5+f_8)-(f_3+f_6+f_7)=u_x=0, \tag{40}$$
$$(f_2+f_5+f_6)-(f_4+f_7+f_8)=u_y=0.$$

Assume the bounce-back rule for the nonequilibrium part of the distribution functions normal to the boundary, namely, in this case,

$$f_2-f_2^{(0)}=f_4-f_4^{(0)}. \tag{41}$$

From (40) and (41), f_2, f_5, f_6, and d can be found as

$$f_2=f_4,$$
$$f_5=f_7-\frac{1}{2}(f_1-f_3),$$
$$f_6=f_8+\frac{1}{2}(f_1-f_3), \tag{42}$$
$$d=f_0+f_1+f_3+2(f_4+f_7+f_8).$$

With (42), the relaxation step can be applied on the boundary nodes as well. Notice that in the present improved model, as f_i is related to momentum (or velocity) by (27), it is not necessarily a conserved quantity on the boundaries.

2. Boundary with prescribed pressure

To cast the boundary condition with a specification of pressure at the inlet and outlet of the channel, we use the following scheme. For simplicity, we consider the case of a node at the inlet [see, e.g., node (1,3) in Fig. 2]. A similar procedure can be applied to the nodes at the outlet. The boundary with specified pressure is supposed to be aligned in the y direction with $\vec{e}_3$, $\vec{e}_6$, and $\vec{e}_7$ pointing outside the system of interest on a node at the inlet (see Fig. 2). After streaming, f_0, f_2, f_3, f_4, f_6, and f_7 are known, while f_1, f_5, and f_8 are unknown. For a node at the inlet, $u_y=0$ is specified and d is also known from Eq. (29) since the pressure is specified. So we have to determine f_1, f_5, f_8, and u_x from (27) as

$$f_0+f_1+f_2+f_3+f_4+f_5+f_6+f_7+f_8=d,$$
$$(f_1+f_5+f_8)-(f_3+f_6+f_7)=u_x, \tag{43}$$
$$(f_2+f_5+f_6)-(f_4+f_7+f_8)=u_y=0.$$

There are four unknowns f_1, f_5, f_8, and u_x, while only three equations are obtained. We assume once again the cancella-

tion for the nonequilibrium part of the momentum distribution in the direction normal to the inlet (outlet) (see Fig. 2),

$$f_1+f_3=f_1^{(0)}+f_3^{(0)}. \tag{44}$$

From (43) and (44), f_1, f_5, f_8, and u_x can be evaluated as

$$\begin{aligned} u_x&=d-[f_0+f_2+f_4+2(f_3+f_6+f_7)],\\ f_1&=f_x-f_3,\\ f_5&=\frac{1}{2}(d-f_0-f_x)-f_2-f_6,\\ f_8&=\frac{1}{2}(d-f_0-f_x)-f_4-f_7, \end{aligned} \tag{45}$$

where

$$f_x=\frac{2(1-\alpha)}{5}d+\frac{2}{3}u_x^2. \tag{46}$$

A corner node at the inlet needs some special treatment. Consider the bottom node at the inlet as an example [see node (1,1) in Fig. 2]. After streaming, only f_0, f_3, f_4, and f_7 are known, while two extra quantities f_2 and f_6, in addition to f_1, f_5, and f_8, are not available from the streaming. Note that the corner node is also a lower boundary node [see node (1,1) in Fig. 2]; $u_x=0$ is therefore specified and the bounce-back rule (41) may be assumed as well. As a result, the five unknown quantities, f_2 and f_6, together with f_1, f_5, and f_8, can be calculated as (45) and (46) with

$$f_2=f_4, \quad f_6=\frac{1}{2}[d-(f_0+f_2+f_4+2f_3+2f_7)]. \tag{47}$$

The top node at the inlet can be handled in a similar way.

Here it is interesting to compare our pressure boundary condition with that proposed in [13], which assumed the bounce-back rule for the nonequilibrium part of the distribution in the direction normal to the inlet (outlet), namely,

$$f_1-f_1^{(0)}=f_3-f_3^{(0)} \tag{48}$$

for nodes at the inlet and outlet instead of (44) in our scheme. Although both schemes are able to recover exactly the analytical results (7) of Poiseuille flow on the square lattice, the bounce-back rule for the nonequilibrium part of the distribution fails to get the exact solution (7) on the triangular lattice. On the other hand, our scheme, which assumes the cancellation rule for the nonequilibrium part of distribution normal to the inlet (outlet), works well on both the square lattice and the triangular lattice.

Finally, it should be emphasized that due to the bounce-back rule (41) used for lower and upper boundaries, the analytical solution of the distribution function (31)–(39) cannot be recovered, although the macroscopic solution (7) of the Navier-Stokes equations (4) and (5) is obtained, accurately up to machine accuracy, by numerical simulation. For τ ranging from 0.65 to 20.0, u_0 ranging from 0.001 to 0.3, and a variety of n_x and n_y, with the use of our boundary conditions, our numerical simulation shows that the f_i evolve into

$$\begin{aligned} &f_0'=f_0, \quad f_1'=f_1, \quad f_3'=f_3,\\ &f_2'=f_2+c_1q^{y/\delta}, \quad f_4'=f_4+c_1q^{-y/\delta}, \quad f_5'=f_5-\frac{1}{2}c_1q^{y/\delta},\\ &f_6'=f_6-\frac{1}{2}c_1q^{y/\delta}, \quad f_7'=f_7-\frac{1}{2}c_1q^{-y/\delta},\\ &f_8'=f_8-\frac{1}{2}c_1q^{-y/\delta}, \end{aligned} \tag{49}$$

where the f_i, with $i=0,1,\ldots,8$, are given by (31)–(39) and

$$q=\frac{\tau-1}{\tau}, \quad c_1=\frac{4}{3}\frac{(6\tau^2-6\tau+1)\delta^3q^{1/\delta}\tau u_0^2}{1-q^{2/\delta}}. \tag{50}$$

With the use of boundary conditions proposed in [13], the f_i evolve into

$$\begin{aligned} &f_0''=f_0', \quad f_2''=f_2', \quad f_4''=f_4',\\ &f_1''=f_1'+c_2q^{x/\delta}, \quad f_3''=f_3'+c_3q^{-x/\delta}, \quad f_5''=f_5'-\frac{1}{2}c_2q^{x/\delta},\\ &f_6''=f_6'-\frac{1}{2}c_3q^{-x/\delta}, \quad f_7''=f_7'-\frac{1}{2}c_3q^{-x/\delta},\\ &f_8''=f_8'-\frac{1}{2}c_2q^{x/\delta}, \end{aligned} \tag{51}$$

where the f_i', with $i=0,1,\ldots,8$, are given by (49) and (50) and

$$c_2=\frac{2}{9}\frac{(1-2\tau)\delta^2\tau u_0}{1+q^{n_x-1}}, \quad c_3=-q^{n_x-1}c_2. \tag{52}$$

Notice that both of the distribution functions [Eqs. (49) and (50) and Eqs. (51) and (52)] recover the macroscopic analytical solution (7) of the Navier-Stokes equations (4) and (5) for steady Poiseuille flow.

IV. SUMMARY

In this paper, we have proposed an improved LBGK model in which the exact form of a 2D steady-state incompressible Navier-Stokes equations can be recovered and the density of the fluid becomes an irrelevant invariant. The improved model is illustrated on a 2D triangular lattice as well as a square lattice. Based on the present scheme, exact analytical solutions to the distributions functions of 2D triangular and square-lattice LBGK models for steady-state Poiseuille flow are obtained. Methods for treating boundary conditions have been presented that can be used to obtain the analytical solutions to the distribution function for numerical simulation on both lattices. On the square lattice, different analytical solutions to the microscopic distribution functions,

due to the implementation of different boundary schemes, have been given. Although distinguished in the microscale scale, these analytical solutions lead to the same macroscopic flow velocity.

We would like to point out that for steady plane Couette flow where the flow is driven by moving the upper boundary with velocity u_c as well as pressure difference, the analytical solutions to the distribution functions of the present LBGK model can be similarly obtained on both the triangular and square lattices. In addition, with the use of the pressure and nonslip boundary conditions proposed here in a numerical simulation, the distribution function f_i will evolve into the analytical solutions, exactly up to machine accuracy, when the simulation becomes stable [16].

It is clear that the results here are just a first stage of the study of incompressible LBGK methods. It is interesting to extend the present approach to the cases of three dimensions. The boundary conditions for complex geometry, especially in three dimensions, will be much more challenging. In addition, it is also important to generalize the incompressible scheme to more general unsteady (time-dependent) flows. The compressibility error-free scheme for unsteady flows is believed to be more useful in simulating the procedure of the displacement of oil in porous media. Work along these lines is in progress.

ACKNOWLEDGMENTS

The authors would like to thank Exxon R&E Company for financial support and Professor Ping Sheng for illuminating discussions.

[1] G. McNamara and G. Zanetti, Phys. Rev. Lett. **61**, 2332 (1988).
[2] F. Higuera and J. Jimenez, Europhys. Lett. **9**, 663 (1989).
[3] S. Chen, H. Chen, D. Martinez, and W. H. Matthaeus, Phys. Rev. Lett. **67**, 3776 (1991); H. Chen, S. Chen, and W. H. Matthaeus, Phys. Rev. A **45**, 5771 (1992).
[4] Y. H. Qian, D. d'Humières, and P. Lallemand, Europhys. Lett. **17**, 479 (1992).
[5] A. K. Gunstensen, D. H. Rothman, S. Zaleski, and G. Zanetti, Phys. Rev. A **43**, 4320 (1991).
[6] D. Grunau, S. Chen, and K. Eggert, Phys. Fluids A **5**, 2557 (1993).
[7] S. Succi, E. Foti, and F. Higuera, Europhys. Lett. **10**, 433 (1989).
[8] A. Cancelliere, C. Chang, E. Foti, D. H. Rothman, and S. Succi, Phys. Fluids A **2**, 2095 (1990).
[9] D. H. Rothman and S. Zaleski, Rev. Mod. Phys. **66**, 1417 (1994).
[10] S. P. Dawson, S. Chen, and G. Doolen, J. Chem. Phys. **98**, 1514 (1993).
[11] Q. Zou, S. Hou, S. Chen, and G. D. Doolen, J. Stat. Phys. **81**, 35 (1995).
[12] Q. Zou, S. Hou, and G. D. Doolen, J. Stat. Phys. **81**, 319 (1995).
[13] Q. Zou and X. He (unpublished).
[14] D. R. Noble, S. Chen, L. G. Georgiadis, and R. O. Buckius, Phys. Fluids A **7**, 203 (1995).
[15] After the submission of this manuscript, we were informed that a paper by S. Chen *et al.*, Phys. Fluids (to be published), presents a more general and model-independent method for treating boundary conditions.
[16] Z. Lin, H. Fang, and R. Tao (unpublished).